A R C H I V E S O F M E T A L L U R G Y A N D M A T E R I A L S
Volume 60 2015 Issue 1
DOI: 10.1515/amm-2015-0026

T. RZYCHOŃ*, B. DYBOWSKI*, A. KIEŁBUS*

# THE INFLUENCE OF STRONTIUM ON THE MICROSTRUCTURE OF CAST MAGNESIUM ALLOYS CONTAINING ALUMINUM AND CALCIUM

# WPŁYW STRONTU NA MIKROSTRUKTURĘ ODLEWNICZYCH STOPÓW MAGNEZU Z DODATKIEM ALUMINIUM I WAPNIA

The structure of Mg-9Al-2Ca-$x$Sr alloys is composed of $\alpha$-Mg grains and the $Al_2Ca$ and $Al_4Sr$ phases in the interdendritic areas. These phases are formed as a result of eutectic reactions. Globular particles of the $Al_8Mn_5$ phase are observed within the interior of the grains. The addition of strontium to Mg-9Al-2Ca-0.4Mn alloys causes the formation of the $Al_4Sr$ phase and increase of its volume fraction with increasing strontium levels. Moreover, increase of the strontium amount causes a decrease of aluminum content in the $\alpha$-Mg solid solution.

*Keywords*: Magnesium alloys, Microstructure, Cast Mg-Al-Ca-Sr Alloys

W artykule przedstawiono wyniki badań wpływu strontu na mikrostrukturę odlewniczych stopów magnezu zawierających aluminium i wapń. Jakościową analizę fazową przeprowadzono za pomocą rentgenowskiej analizy fazowej i metody EBSD. Do ilościowej analizy fazowej zastosowano metody analizy obrazu. Po odlewaniu mikrostruktura stopów zawierających 9% mas. aluminium, 2% mas. wapnia, 0,3% mas. strontu i 0,4% mas. manganu składa się z roztworu stałego $\alpha$-Mg oraz wydzieleń faz międzymetalicznych $Al_2Ca$, $Al_4Sr$ i $Al_8Mn_5$. Zwiększenie zawartości strontu do 2% mas. powoduje zwiększenie udziału objętościowego fazy $Al_4Sr$ i zmniejszenie stężenia aluminium w roztworze stałym $\alpha$-Mg.

## 1. Introduction

Magnesium alloys are among the lightest structural materials. Their relatively low density in combination with satisfactory mechanical and casting properties cause them to be widely used in the automotive and aviation industries [1,2]. In the case of the common Mg-Al alloys, the mechanical properties are dramatically reduced above 120°C [3]. Thus, it becomes necessary to develop magnesium alloys which could operate at elevated temperatures. The very promising results are achieved for Mg-Al alloys containing rare-earth. They possess the ability to withstand in temperature up to 200°C. The disadvantage of these alloys is their relatively high cost due to the presence of expensive rare-earth metals [4-7]. A good alternative for Mg-Al-RE alloys are the newest Mg-Al-Ca alloys. Calcium exerts a positive effect on the creep resistance of Mg-Al alloys. Moreover, calcium boasts the low density and cost [2]. The creep resistance of Mg-Al-Ca alloys may be also improved by the addition of strontium. Content of approx. 1 wt. % of strontium in the Mg-5Al-3Ca alloy enables the increase of the creep resistance at ambient and elevated temperature due to solid solution strengthening [8]. Aluminum in Mg-Al-Ca alloys improves the mechanical properties at ambient temperature and casting properties. Manganese increases corrosion resistance in a saline environment [3,4,5]. The composition of the phases of Mg-9Al-2Ca alloys and the level of dissolved aluminium in the solid solution both play a key role in the increase of creep resistance in Mg-Al-Ca-Sr alloys. Therefore, the purpose of the present work is to describe the influence of strontium on the phase composition, volume fraction of compounds and aluminum content in magnesium solid solution.

## 2. Materials and experimental procedures

In the present work three magnesium alloys containing aluminum, calcium, strontium and manganese were produced. Chemical composition of the investigated alloys, determined by X-ray fluorescence spectroscopy, is given in the Table 1. Commercial pure Mg, Al and Mn were used, strontium and calcium were added in the form of Al-10 wt.% Sr and Al-85 wt% Ca master alloys, respectively. Melting of the alloys was conducted by induction melting in an $Al_2O_3$ crucible under the protection of an argon atmosphere. The melt was held at 730°C for 3 min then poured into sand moulds.

TABLE 1
Chemical composition of investigated alloys [wt. %]

| Alloy | Mg | Al | Ca | Mn | Sr |
|---|---|---|---|---|---|
| Mg-9Al-2Ca-0.4Mn-0.3Sr | Balance | 8.9 | 2.1 | 0.3 | 0.3 |
| Mg-9Al-2Ca-0.4Mn-1.4Sr | Balance | 9.3 | 2.2 | 0.4 | 1.4 |
| Mg-9Al-2Ca-0.4Mn-2Sr | Balance | 9.1 | 1.7 | 0.5 | 1.9 |

* SILESIAN UNIVERSITY OF TECHNOLOGY, KATOWICE, POLAND

Microstructural investigation of the alloys studied was carried out using light microscopy and scanning electron microscopy (SEM). The samples were mechanically polished and etched in acetic glycol. Microanalysis of intermetallic compounds was performed by means of energy dispersive X-ray spectroscopy (EDS). Phase identification was performed by electron back-scatter diffraction (EBSD) and X-ray diffraction (XRD) methods. The images used for the quantitative evaluation of the microstructure were recorded with use of the Olympus GX71 light microscope using bright field technique with a magnification of ×1000. The analysis was conducted on a sample material area equal to 0.347 $mm^{2}$. Estimation of stereological parameters was performed using the Met-Ilo v. 12.1 program.

In order to ensure the correct detection of the two types of intermetallic phases (the lamellar phase and the coarse phase), a macroinstruction based on the varying gray levels was elaborated. After the normalisation of the input image, the top and bottom binary thresholds were selected manually. The next step involved a binary segmentation and phase reconstruction (Fig. 1a). In order to avoid areas of the $\alpha$-Mg solid solution which were to be found inside the eutectic areas, the 'top hat' operation was performed – based on the detection of locally lighter areas [6] (Fig. 1b).

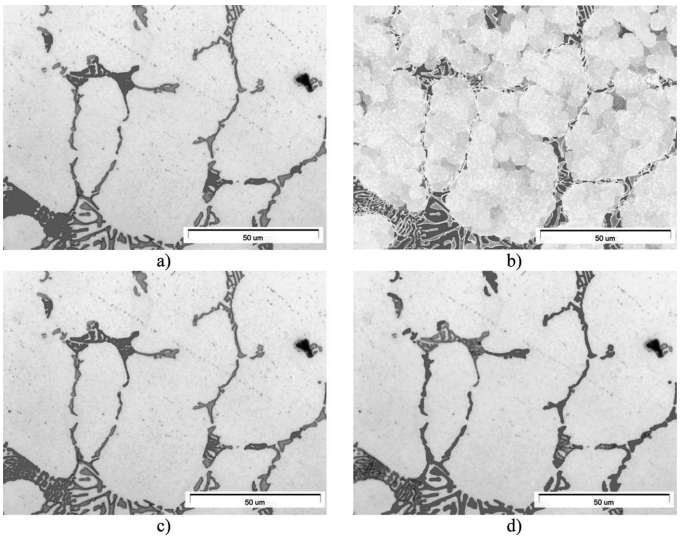


Fig. 1. The procedures used to determination of the volume fraction of the intermetallic phases: a) final image after set of operations used for binarization of the darker phase ($Al_4Sr$ phase); b) binarization of the locally brighter areas in the input image; c) image used for the analysis of darker phase; d) image used for the analysis of brighter phase ($Al_2Ca$ phase)

The final image used for the quantitative evaluation of the lamellar phase – after an appropriate series of algebraic operations and manual correction – is presented in Fig. 1c. The detection of the coarse eutectic phase (Fig. 1d) is based on the subtraction of the binary image of the lamellar phase from the final binary image. The volume fraction of compounds was calculated from the Cavalieri relation: $V_V = A_A = L_L$, where $V_V$ – volume fraction, $A_A$ – area fraction, $L_L$ – linear fraction [1].

## 3. Results

The investigated alloys exhibit dendritic microstructure. Light microscopy investigations revealed that the microstructure consists of the $\alpha$-Mg solid solution dendrites and precipitates of intermetallic phases distributed in interdendritic areas. Moreover, the globular particles are present inside the $\alpha$-Mg solid solution (Fig. 2). SEM analysis showed the presence of three phases with varied morphology and chemical composition. The interdendritic lamellar phase is rich in aluminum and strontium (Fig. 3, pt. 1). The irregular shape compound contains mainly aluminium and calcium (Fig. 3 pt. 2). The globular particles found within the dendrites of the $\alpha$-Mg solid solution are composed of aluminium and manganese (Fig.3, pt.3) Within the $\alpha$-Mg solid solution, a small number of plate-like precipitates enriched with calcium was also observed. It should be emphasised that all the analysed precipitates are characterised by an increased content of magnesium due to the interaction of the electron beam with the magnesium matrix. The X-ray diffraction analysis (Fig. 4) was used in order to identify the phase composition of the investigated alloys. It was confirmed that all the alloys examined contain the $\alpha$-Mg solid solution and the $Al_2Ca$ Laves phase with the C15 crystal structure which can contain also magnesium and strontium. Moreover, the lamellar phase was identified as the $Al_4Sr$ compound, which is capable of dissolve calcium up to approximately 1.5% at. The globular particles containing manganese were not identified by the X-ray diffraction due to their small volume fraction. However one weak diffraction line at 42.5° $2\theta$ (Fig. 4) is observed, which can correspond to $Al_8Mn_5$ phase. The presence of the $Al_4Sr$ and $Al_2Ca$ phases has also been confirmed by the EBSD method (Figs. 5 and 6).

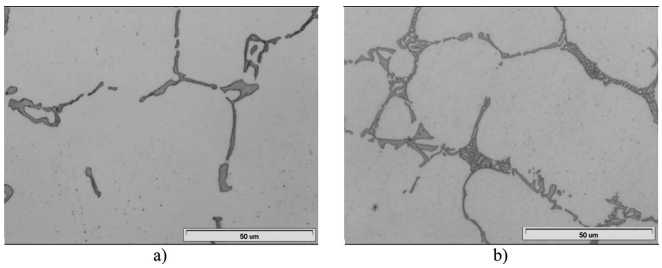


Fig. 2. The microstructure of a) Mg-9Al-2Ca-0.4Mn-0.3Sr and b) Mg-9Al-2Ca-0.4Mn-2Sr alloys, LM

The average aluminum content in the $\alpha$-Mg solid solution determined by the EDS point analysis is presented in Table 2. It can be seen that an increased level of strontium in the investigated alloys causes a decrease in aluminium content in the $\alpha$-Mg solid solution.

The results of the quantitative evaluation of the microstructure are presented in Table 3. It can be concluded that the volume fraction of the $Al_2Ca$ (C15) and $Al_8Mn_5$ phases is not dependent on the strontium content in the investigated alloys. However, the volume fraction of the $Al_4Sr$ phase and the total amount of the intermetallic compounds rise with the increase of the strontium content in Mg-Al-Ca-Mn alloys.

## 4. Discussion

The cast Mg-Al-Ca and Mg-Al-Ca-Sr alloys have been extensively investigated in recent years. It was determined that the addition of calcium improves the creep resistance of Mg-Al alloys. This is due to the formation of intermetallic compounds with a high melting point in comparison with the $Mg_{17}Al_{12}$ phase, which plays a crucial role in the strengthening of binary Mg-Al alloys. In Mg-(5÷9)Al-(1÷3)Ca alloys, three kinds of intermetallic compounds may formed directly after solidification: the $Mg_2Ca$ phase with the hexagonal C14 type crystal structure, the $Al_2Ca$ phase with the cubic C15 type structure or the $(Mg,Al)_2Ca$ phase with the hexagonal C36 type crystal structure [9]. Among these Laves compounds, the $Al_2Ca$ phase exhibits the highest structural stability, whereas $Mg_2Ca$ possesses the lowest structural stability [10]. Thus, the phase composition of Mg-Al-Ca alloys significantly influences the creep resistance. According to Liang et al. [9], the $Al_2Ca$ (C15) phase may be found in Mg-Al-Ca alloys with a 0.23 Ca/Al ratio. The increase in the Ca/Al ratio to the level of 0.32 results in the $(Mg,Al)_2Ca$ phase becoming the main intermetallic phase in the alloy. In alloys with a 0.54 Ca/Al ratio, the $(Mg,Al)_2Ca$ and $Mg_2Ca$ phases can coexist. However, data derived from scientific publications is ambiguous. According to Suzuki et al. [11], the microstructure of the Mg-Al-Ca alloys may contain only $(Mg,Al)_2Ca$ (C36) and (or) $Mg_2Ca$ (C14) phases after solidification. The $Al_2Ca$ (C15) does not form in these alloys during crystallization.

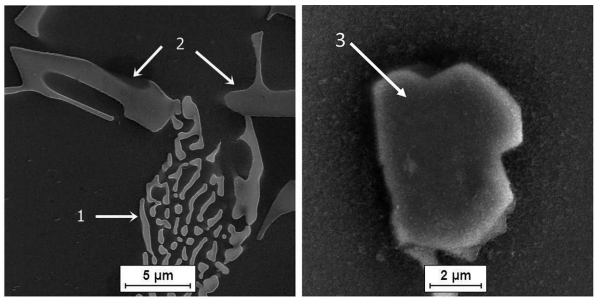


| Point | Chemical composition, %at. | | | | | |
|---|---|---|---|---|---|---|
| | Mg | Al | Ca | Sr | Mn | Phase |
| 1 | 31.3 | 53.5 | 3.2 | 12.0 | | $Al_4Sr$ |
| 2 | 30.0 | 49.9 | 18.9 | 1.2 | | $Al_2Ca$ |
| 3 | 12.3 | 45.6 | | | 42.2 | $Al_8Mn_5$ |

Fig. 3. EDS results of precipitates in investigated alloys (as an example of Mg-9Al-2Ca-0.4Mn-1.4Sr).

In this paper presence of $Al_2Ca$ phase was confirmed by XRD analysis and EBSD method. Moreover, the EDS results showed that this compound possesses the ability of dissolving strontium in quaternary Mg-Al-Ca-Sr alloys. The maximum concentration of Sr in the $Al_2Ca$ phase reaches 2% at. and is not dependent on the strontium content in Mg-9Al-2Ca-$x$Sr alloys. Due to the fact that strontium is characterised by a larger atomic radius than calcium, its presence in the C14 crystal structure should cause an increase of the $a_0$ crystal lattice parameter. This is mirrored in the results of the X-ray phase analysis where the diffraction lines of $Al_2Ca$ phase are slightly shifted towards higher $2\theta$ angles. Apart from being dissolved in the $Al_2Ca$ phase, strontium also forms the $Al_4Sr$ phase which is a characteristic phase in Mg-Al-Sr alloys [1].

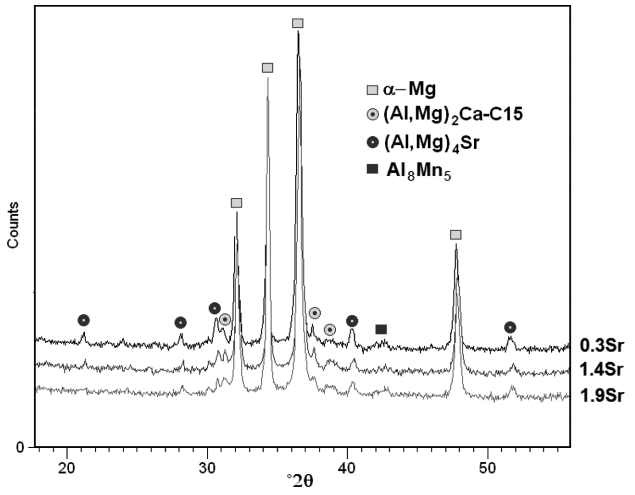


Fig. 4. XRD patterns of investigated alloys

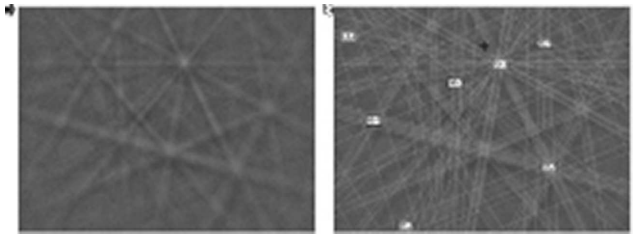

Fig. 5. Experimental EBSD pattern obtained from the irregular-shaped phase solved as $Al_2Ca$ (cubic crystal structure), MAD = 0.46°, spec. plane $(6\bar{4}\bar{5})$

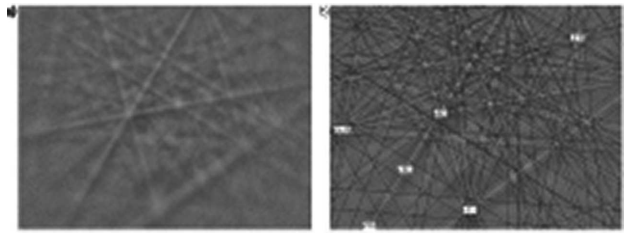

Fig. 6. Experimental EBSD pattern obtained from the irregular-shaped phase solved as $Al_4Sr$ (tetragonal crystal structure) MAD = 0.59°, spec. plane $(\bar{5}\bar{1}0)$

TABLE 2
The average and standard deviation (from six points) of aluminum content in the $\alpha$-Mg solid solution

| | Mg-9Al-2Ca-0.4Mn-0.3Sr | Mg-9Al-2Ca-0.4Mn-1.4Sr | Mg-9Al-2Ca-0.4Mn-2Sr |
|---|---|---|---|
| The Al content in the $\alpha$-Mg [% at.] | 3.2±0.3 | 2.9±0.3 | 2.6±0.2 |

In the tested alloys, calcium may be dissolved in the $Al_4Sr$ phase in amount reaching maximum of 3.5% at. In Mg-Al-Ca-Sr alloys with lower aluminum content (e.g. 4÷6 wt.%), strontium forms the $Al_3Mg_{13}Sr$ [1] or $Mg_{17}Sr_2$ [8] phases. The increase of aluminium levels to 9 wt.% favours the formation of the $Al_4Sr$ phase. The changes in strontium content (within a range of up to 2 wt.%) in alloys containing 9% Al and 2% Ca does not influence on the volume fraction of this phase.

TABLE 3
The results of quantitative analysis of microstructure of the tested alloys

| | Stereological parameters | 0.3Sr | 1.4Sr | 2Sr |
|---|---|---|---|---|
| $Al_2Ca$ | Area fraction $A_A$[%] | 4.8 | 5.1 | 4.7 |
| | Variation coefficient of $A_A\upsilon(A_A)$ [%] | 40 | 27 | 49 |
| $Al_4Sr$ | Area fraction $A_A$[%] | 0.8 | 1.5 | 3.2 |
| | Variation coefficient of $A_A\upsilon(A_A)$ [%] | 55 | 67 | 63 |
| $Mn_8Al_5$ | Area fraction $A_A$[%] | 0.14 | 0.16 | 0.15 |
| | Variation coefficient of $A_A\upsilon(A_A)$ [%] | 128 | 171 | 151 |
| | Shape factor $\xi$ [-] | 0.82 | 0.84 | 0.83 |
| | Variation coefficient of $\xi\upsilon(\upsilon(A_A)$ [%] | 13 | 12 | 12 |

An increase of strontium content causes a growth of the $Al_4Sr$ phase volume fraction and a decrease in aluminium content in the $\alpha$-Mg solid solution. The decrease of the amount of aluminium dissolved in the matrix stems from the increased total volume fraction of the $Al_2Ca$ and $Al_4Sr$ phases, which consume aluminium atoms. Taking into consideration the operation of Mg-Al-Ca-Sr alloys in temperatures up to 180°C, the concentration of aluminium in the $\alpha$-Mg solid solution should not exceed 2.5% at. [4]. Above this content level, precipitation processes of the $Mg_{17}Al_{12}$ phase become possible. This has a negative influence on creep resistance. Aluminium levels should not be too low either, due to the fact that its presence in the crystal lattice of the $\alpha$-Mg causes solution strengthening.

*Received: 20 March 2014.*

**Acknowledgements**

The present work was supported by the Polish Ministry of Science and Higher Education under the strategical project No. POIG.01.01.02-00-015/09 (FSB-71/RM3/2010).

REFERENCES

[1] B. Jing, S. Yangshan, X. Shan, X. Feng, Z. Tianbai, Mater. Sci. Eng. **A 419**, 181-188 (2006).
[2] E. Aghion, B. Bronfin, F. Von Buch, H. Friedrich, S. Schumann, JOM **55(11)**, 30-33 (2003).
[3] K.U. Kainer, Magnesium Alloys and Technologies, Wiley-VCH 2003.
[4] ASM Speciality Handbook, Magnesium and magnesium alloys, ASM International 1999.
[5] T. Rzychoń, J. Szala, A. Kiełbus, Arch. Metall. Mater. **57**, 254-262 (2012).
[6] L. Wojnar, K.J. Kurzydłowski, J. Szala, Praktyka analizy obrazu, Polskie Towarzystwo Stereologiczne, Kraków 2002.
[7] T. Rzychoń, A. Kiełbus, Arch. Metall. Mater. **53**, 901-907 (2008).
[8] A. Suzuki, N.D. Saddock, L. Riester, E. Lara-Curzio, J.W. Jones, T.M. Pollock, Metall. Mater. Trans. A **38A**, 420-427 (2007).
[9] S.M. Liang, R.S. Chen, J.J. Blandin, M. Suery, E.H. Han, Mater. Sci. Eng. **480**, 365-372 (2008).
[10] D.W. Zhou, J.S. Liu, P. Peng, L. Chen, Y.J. Hu, Mater. Lett. **62**, 206-210 (2008).
[11] A. Suzuki, N.D. Saddock, J.W. Jones, T.M. Pollock, Acta Mater. **53**, 2823-2834 (2005).